Progress In Electromagnetics Research, Vol. 161, 113–123, 2018

Efficiency of Millimeter Wave Mobile Terminal Antennas with the Influence of Users

Rizwan Khan, Azremi A. Al-Hadi*, and Ping Jack Soh

Abstract—The effect of users on the efficiency of mobile terminal antennas at 15 GHz, 28 GHz and 60 GHz is studied in this paper. It is performed using three four-element planar arrays. The first operates at 15 GHz with a bandwidth of 0.74 GHz, the second at 28 GHz with a bandwidth of 2.5 GHz and finally the third antenna at 60 GHz with bandwidth of 12.5 GHz. The effect of a user's finger is studied when being placed on four different locations over each antenna element, with six distances between the antenna and user's index finger. The losses due to the increased shadowing are studied in terms of radiation efficiency (RE), matching efficiency (ME) and two additional multiple-input-multiple-output (MIMO) parameters, i.e., envelop correlation coefficient (ECC) and multiplexing efficiency (MUX). For antennas operating at 28 and 60 GHz, the minimum frequency shift is observed when the finger is placed at 1.5 mm distance from the antenna, whereas for 15 GHz, the minimum resonance shift is observed when the finger is at 2 mm distance. Losses of up to 80% and 70% are observed for RE and MUX, respectively, when the finger is placed at 0 mm for all antennas compared to the case without user (WU). Finally, it is observed that the ME and ECC losses are insignificant regardless of the antenna and finger variation.

1. INTRODUCTION

With rapidly increased number of mobile communication users, the spectrum resources in the current cellular band (below 6 GHz) are insufficient to satisfy the increasing demand on data throughput. Therefore, the advancement in millimeter-wave (mmWave) technologies, coupled with large amount of available spectrum have triggered exponential interest in the mmWave band (10 GHz to 200 GHz) for the next generation 5G mobile communication purposes [1]. Realizing this, FCC introduced a new set of spectrum allocation in the frequencies of 28 GHz, 37 GHz, 39 GHz and 64 to 71 GHz (FCC 15138) [2].

Antennas and devices operating at mmWave bands are intrinsically compact compared to their counterparts in the lower microwave spectrum. Moreover, the communication link at mmWave band is inherently secure and features less interference among users. However, communication distances in the mmWave frequency bands are limited by a high attenuation caused by the atmosphere absorption [3]. Besides that, the tighter fabrication tolerance, higher material losses, and packaging issue in the mmWave bands often hinder the performance of wireless networks [4]. Therefore, high gain and wide bandwidths are required for the antennas in mmWave communication, which promise high-data-rate wireless communication [5].

According to the Friis equation, the higher frequency used in communication suffers from greater path loss, resulting in smaller cell coverage in mmWave communication. In addition to that, wireless transmissions in this band are susceptible to shadowing due to the human body obstructing the line-of-sight path [6] and generate a large fluctuation on the received signal strength of the user equipment [7].

Received 24 January 2018, Accepted 24 March 2018, Scheduled 20 April 2018

* Corresponding author: Azremi Abdullah Al-Hadi (azremi@unimap.edu.my).
The authors are with the Advanced Communication Engineering (ACE) Centre of Excellence, School of Computer and Communication Engineering, Universiti Malaysia Perlis, Kangar, Perlis 01000, Malaysia.

Shadowing losses, along with increased path loss and multipath can be mitigated by using directional antennas [8]. To address these challenges, beamforming has been proposed as one of the methods to overcome the path loss at both mobile and base station in such high frequencies [9]. Several antenna types considered for end users mobile devices at mmWave frequencies have been aimed at providing beam steerable antenna array and high gain. Beside gain, several phased antenna arrays for mmWave have been proposed in [10, 11], and an investigation of human body effects at 15 GHz using a phased array is presented in [12]. Moreover, antennas in the mmWave frequency needs to be able to be integrated in or collocated in proximity of the RF transceiver [13].

Besides the antenna characteristics, another aspect that needs to be investigated in mmWave mobile application is the effect of users. This is to ensure that the effects of users on mobile terminal antennas for 5G communication systems can be properly estimated. This paper investigates the effects of user finger's loading on the performance of mobile terminal antenna at 15, 28 and 60 GHz using simulations. For the first time, to the best of the authors' knowledge, this is performed in terms of RE, ME, ECC, and MUX using user's index finger for these frequencies. First, detailed antenna designs will be presented, followed by the effects of finger loading on antenna scattering parameters. Next, the results of RE and ME for all antennas with different index finger locations will be discussed, prior to several concluding remarks.

2. PLANAR 4-PORT ANTENNAS FOR 15/28/60 GHZ MOBILE TERMINAL

2.1. Antenna Configuration

The proposed array designs for 15, 28, and 60 GHz are printed on a same Rogers (RO3003) substrate with relative permittivity $\varepsilon_r = 3$, loss tangent 0.0013, and thickness 0.13 mm. The substrate for all 15, 28, and 60 GHz mobile terminal antennas is sized at $55 \times 110\,\text{mm}^2$ as illustrated in Figures 1(a), (b), and (c), respectively. To ensure a fair comparison, several design strategies are outlined. Firstly, the radiating element of the array is located on the same (fully metalized) side of the substrate, with their radiator designed inside a slotted area of size $2.2 \times 5.3\,\text{mm}^2$. Secondly, the edge-to-edge distance in each slotted area (where each antenna element (AE) is located) is standardized to $\lambda/2$. Next, a same feeding mechanism is utilized: a 50 Ω transmission line on the reverse side of the substrate. Power is then fed to the radiating elements by connecting this transmission line using a metallic via of radius 0.14 mm. To enable specific resonances, an inverted C-shape is used as the 15 GHz antenna. Meanwhile, the 28 GHz antenna is designed based on a rectangular-based patch chamfered at two of its edges (by 0.55 mm). Finally, the 60 GHz array is formed by using four L-shaped radiators, see Figure 1(c).

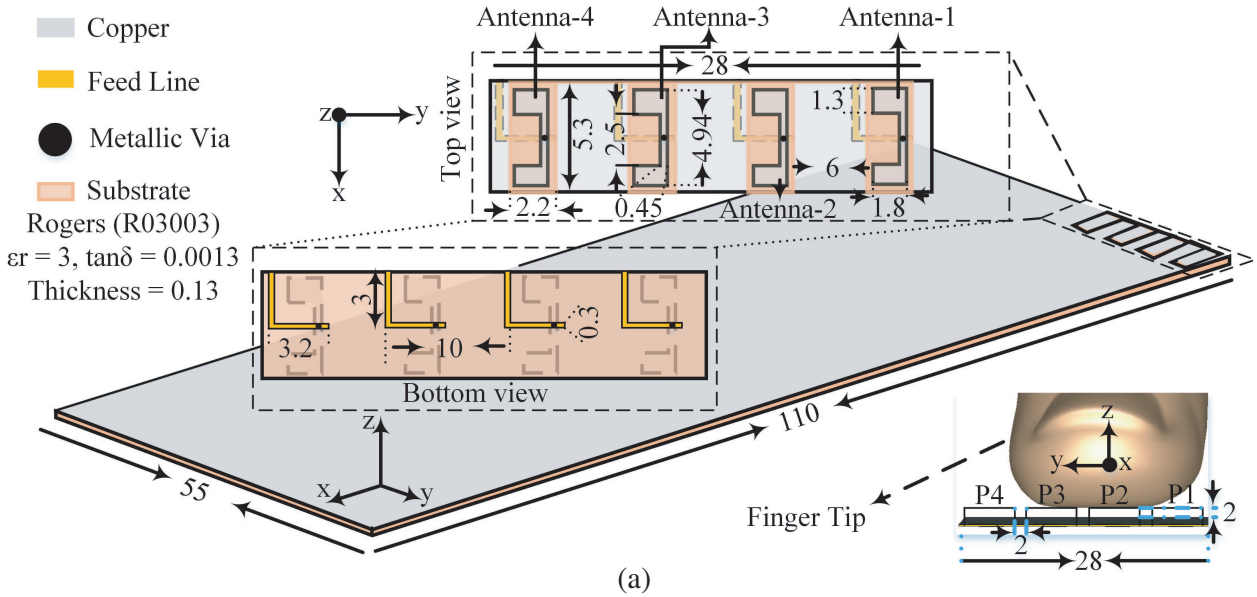

(a)

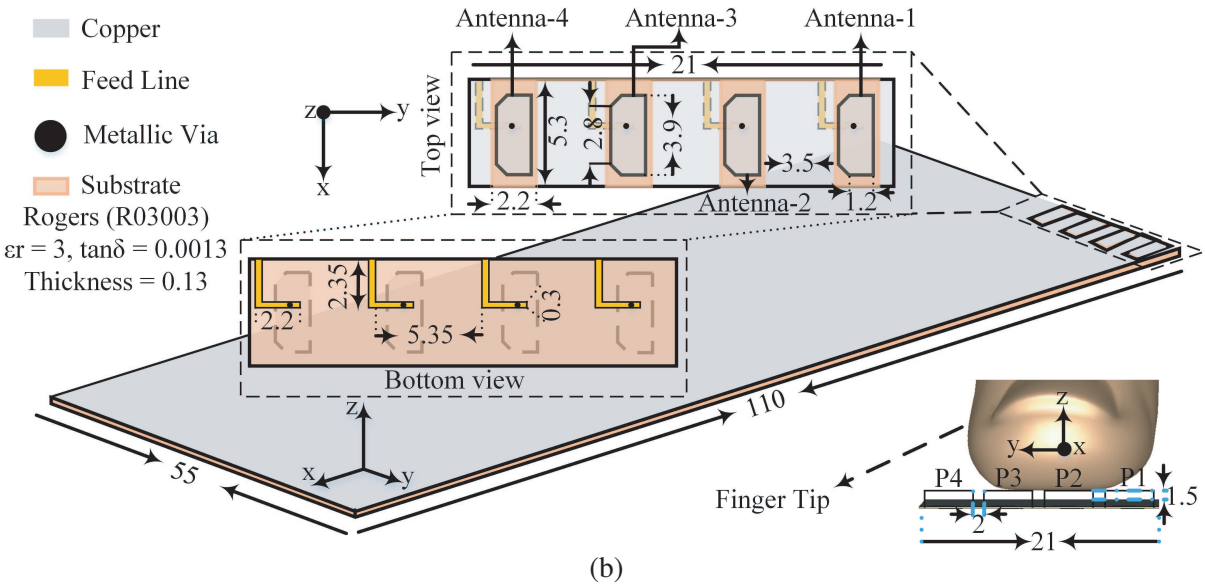

(b)

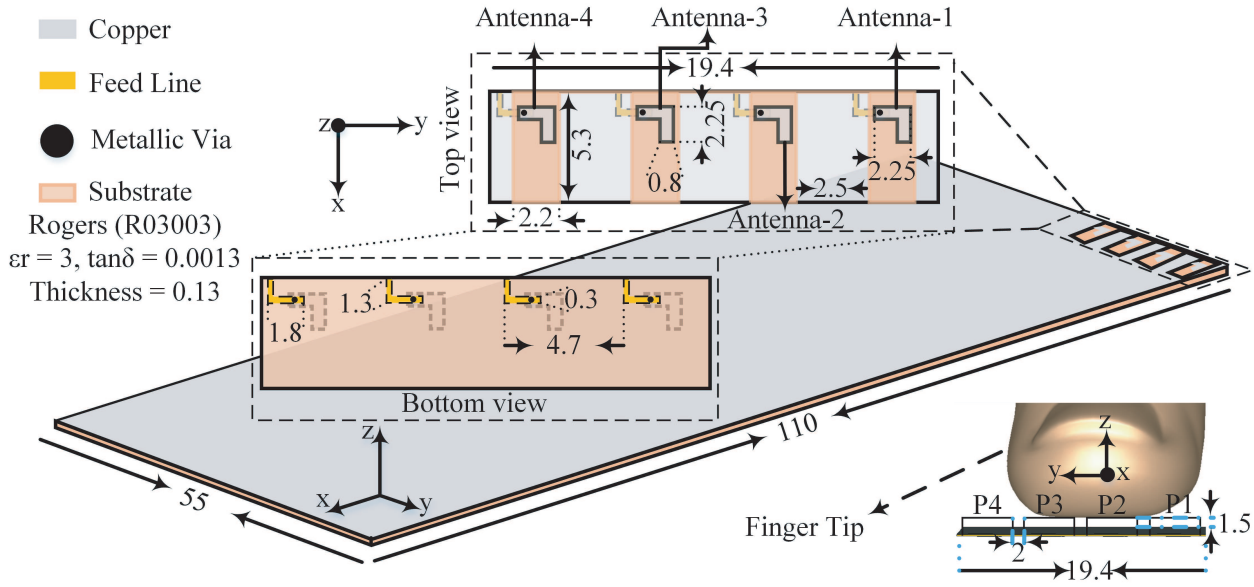

(c)

Figure 1. Antenna geometry for the (a) 15 GHz, (b) 28 GHz, and (c) 60 GHz array and the index finger placement. All dimensions are in millimeter.

Due to the large amount of computational resources required to simulate a user hand above 15 GHz, a finger is used to simplify this study. To study the effects of this finger, a 3D model of a user's index finger was used (see Figure 1(a) to Figure 1(c)). The dimensions of the index finger were 12 mm in height, 78 mm in length, and 17 mm in width. For all antennas, the finger model is placed at four different positions (P1, P2, P3, and P4) on top of each antenna element (see Figure 1(a) to Figure 1(c)). The tissue properties of the finger phantom are defined using ε_r and conductivity (ρ) as follows: 15 GHz ($\varepsilon_r = 31$; $\rho = 18.8$ S/m), 28 GHz ($\varepsilon_r = 18.9$; $\rho = 31.91$ S/m) and 60 GHz ($\varepsilon_r = 7.98$; $\rho = 36.38$ S/m) [14].

2.2. Antennas Scattering Parameters

All simulations were performed using the time domain solver in CST microwave studio software. The reflection coefficients (S_{11}) of the single antenna element designed for 15, 28 and 60 GHz are similar in free space (FS) due to their symmetry. Only S_{11} for Antenna-1 in the 15, 28, and 60 GHz arrays and their inter-element isolations (S_{12}, S_{13}, S_{14}, S_{23}, S_{24} and S_{34}) are presented in Figures 2(a), (b) and (c). It is observed that the maximum inter-element isolation for the scenario without user (WU) is −20 dB, −21 dB and −23 dB for 15, 28, and 60 GHz, respectively.

The user finger is simulated on top of Antenna-1 from 15, 28 and 60 GHz arrays at six different heights, and their S_{11} are shown in Figures 3(a), (b) and (c). The behaviors of all other antenna elements (Antenna-2, 3 and 4) are found similar. Severe upwards resonance shifts are observed when the finger is placed with less than 2 mm distance from the antenna for the 15 GHz array, and less than 1.5 mm for 28 and 60 GHz arrays. On the contrary, minimum shifts of up to 0.22 GHz, 0.1 GHz and 0.15 GHz are observed for 15, 28 and 60 GHz, respectively, when the distance of the user finger above the antenna element is 1.5 mm. This value remains almost constant despite varying distances up to 2.5 mm with fluctuations in matching. Previous researchers also observed that at mmWaves, an air gap of 0 to 2 mm between the antennas and human skin decreases the transmission [15]. Figures 4(a), (b) and (c) show the antenna's S-parameters with the finger placed at 2 mm for 15 GHz, and 1.5 mm for 28 GHz and 60 GHz from it (with finger placement P1).

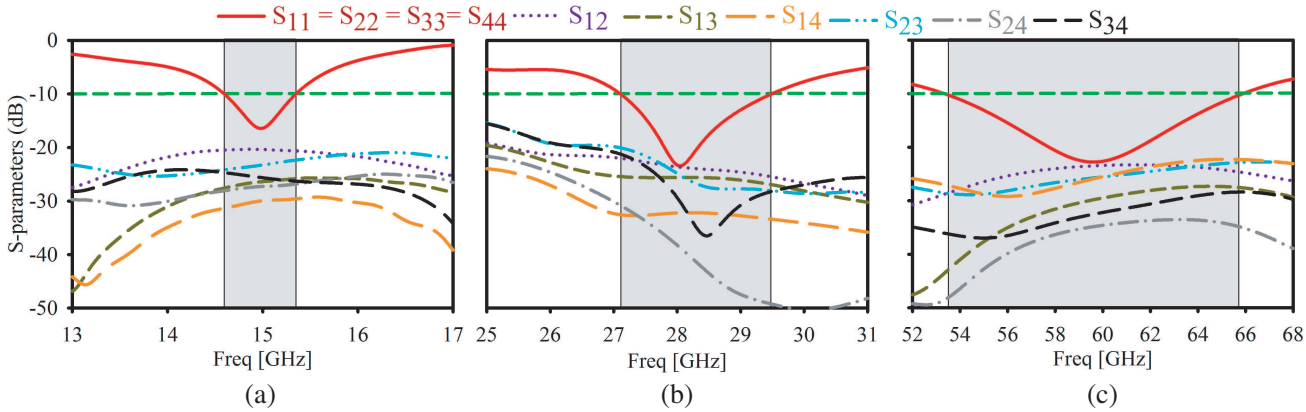

Figure 2. Antenna S-parameters for (a) 15 GHz, (b) 28 GHz, and (c) 60 GHz.

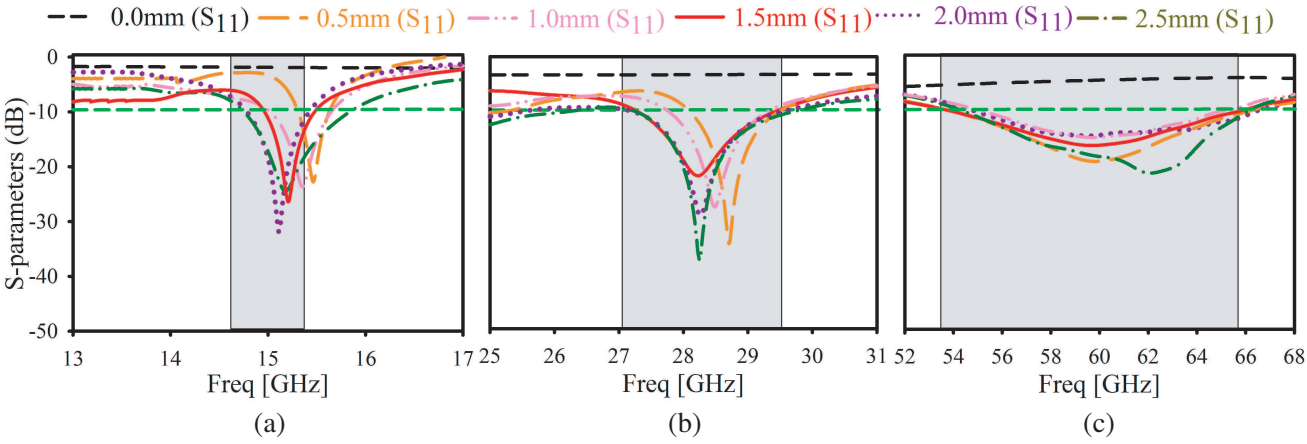

Figure 3. S-parameters with user's finger at different distances on top of Antenna-1: (a) 15 GHz, (b) 28 GHz, and (c) 60 GHz.

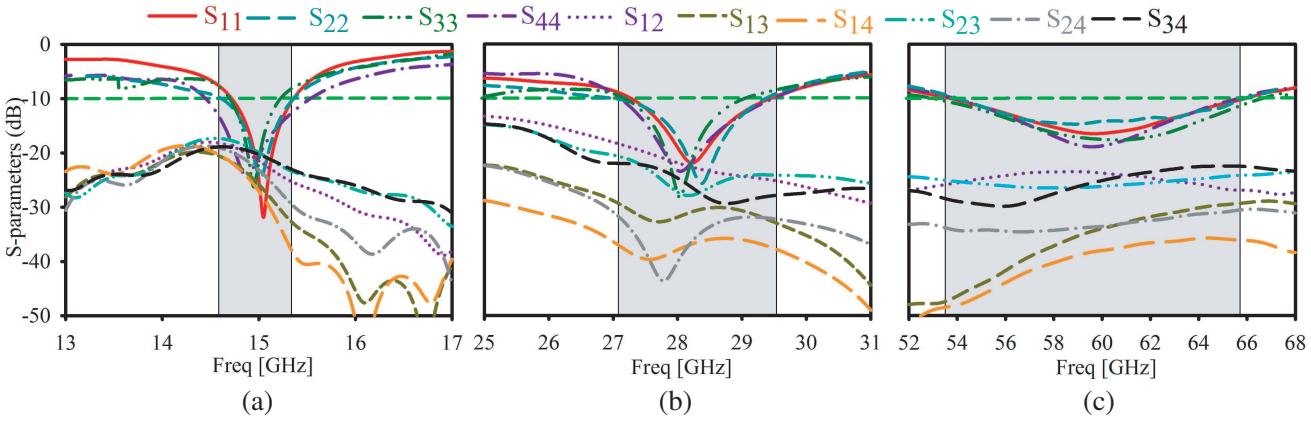

Figure 4. S-parameters when index finger at P1, showing (a) 15 GHz (b) 28 GHz, and (c) 60 GHz.

3. IMPACT OF USERS ON ANTENNA ELECTROMAGNETIC RADIATION CHARACTERISTIC

Users may hold the mobile in varying methods, and the degree of the hand impact depends on the antenna (size, design, near-field distribution and location) and the grip (position of the finger w.r.t. the antenna, obstructed antenna area and palm-handset distance). The implementation of more than one antenna enables the use of alternate antennas in the event that one of the intended antenna is significantly affected by the user. A realistic finger phantom is simulated at 15, 28 and 60 GHz when being aligned along the y-axis so that the tip of the finger lies on the center of the antenna element. The effect of the finger's distance (in the z-axis) is then studied parametrically from 0 to 2.5 mm for all antennas, with a specific focus on the variation in RE and ME.

3.1. Effect of User's on Antenna Radiation Efficiency

Accurately determining antenna efficiency using full wave simulator is not straightforward due to the material losses and mismatches besides the inaccuracies of conventional pattern computation methods [14]. This is because the losses in the medium that affects the wave in the far-field region attenuate more rapidly and finally become zero. Antenna performance degradation caused by the proximity of the user's finger is expected due to the existence of lossy materials within the antenna near field [16]. In this work, the behaviors of efficiency in the mmWave bands (15, 28 and 60 GHz) are studied by placing a user's index finger on top of the antenna element for all three antenna cases at four different locations. The efficiencies extracted from each antenna element within its 10-dB bandwidth are averaged in this study. Figures 5(a), (b) and (c) show the average RE for all arrays with different finger distances along the z-axis (on top of antenna element). It is shown that with the increase in the separation distance, RE is gradually increased. At least 2 mm separation between the antenna and finger is required at 15 GHz, while a 1.5 mm distance is needed at 28 and 60 GHz. These separations allowed these antennas to radiate moderate energy (larger than 40%) which are considered as an acceptable range for 5G massive MIMO application [3, 17]. Beyond these distances, small amounts of RE improvements are observed. These worst-case distances of 2 mm (at 15 GHz) and 1.5 mm (at 28 and 60 GHz) are chosen to be further analyzed for all antennas cases. This is due to the decoupling of the finger and its losses from the reactive near field of the antenna.

Figures 6(a), (b) and (c) show the average RE for 15, 28 and 60 GHz, respectively, when the index finger is placed at distance of 2 mm (15 GHz) and 1.5 mm (for 28 and 60 GHz) above the antenna elements at four different locations (P1, P2, P3, and P4). The variation of user's finger is done by moving it on the vertical axis of the chassis in 2 mm interval for all antenna cases (see Figures 1(a), (b), and (c)). As expected for the WU cases, the average RE for each antenna element is observed to be about 80% for 15 GHz, and 95% for both 28 and 60 GHz antennas due to the low losses in the RO3003

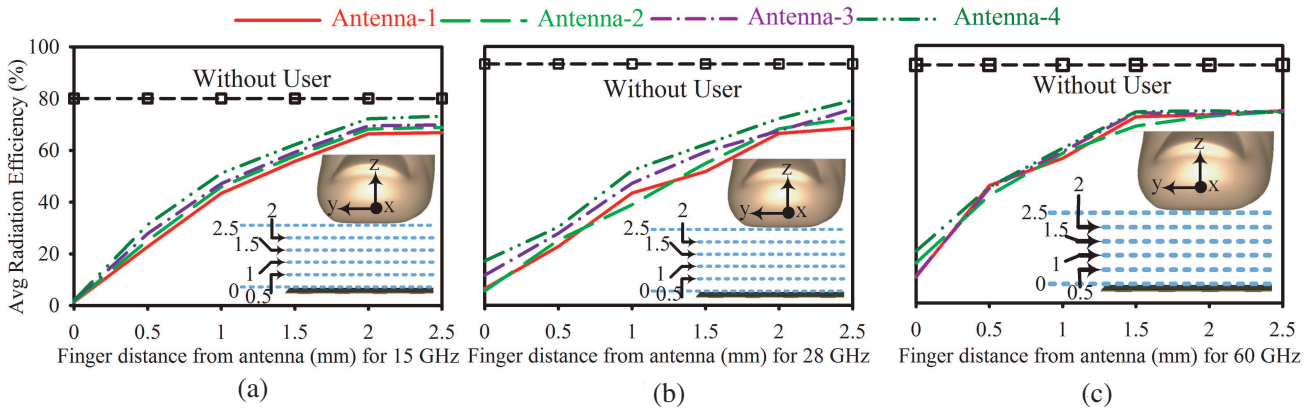

Figure 5. Average radiation efficiency with the variation of the distances between the antenna and the index finger: (a) at 15 GHz, (b) at 28 GHz, and (c) at 60 GHz.

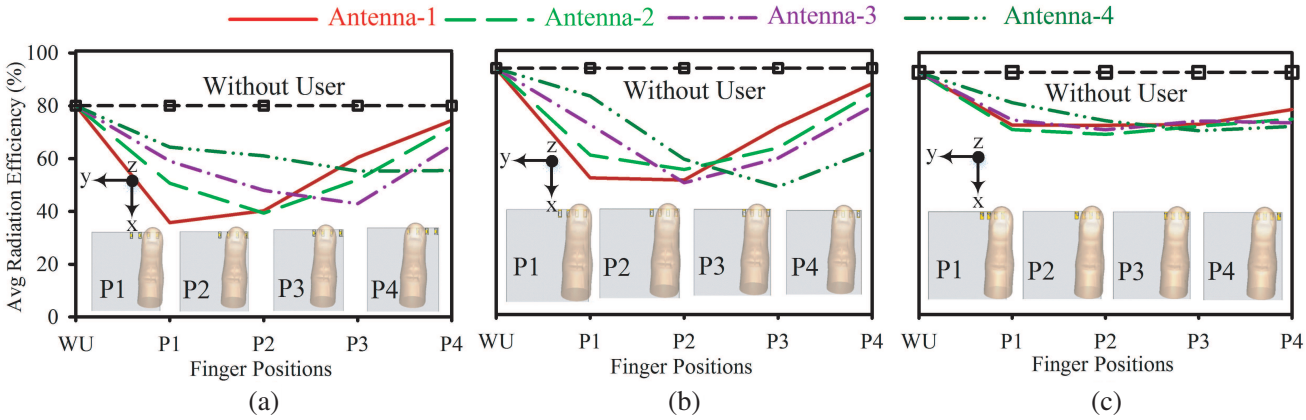

Figure 6. Average radiation efficiency with the variation of finger position: (a) 2 mm at 15 GHz, (b) 1.5 mm at 28 GHz, and (c) 1.5 mm at 60 GHz.

substrate. As the finger location is varied along the negative y-axis, the RE is gradually increased relative to the WU scenario, especially for those antennas which are furthest from the index finger. RE is decreased immediately when the user's finger is placed exactly on top of the antenna element due to the shadowing effect.

From this study it is observed that the RE at mmWave bands is severely affected when the antenna is in close proximity to the user. Two solutions can be used to mitigate the degradation of RE. The first is to design a radome over the antenna element with an appropriate distance. This is expected to create more clearance between the radiating antenna element and the user in the future user's devices. The second method is to increase the number of antenna elements. However, this technique must be implemented with care as to not allow mutual coupling between the antenna elements to further degrade the antenna performance.

3.2. Effect of User's on Antenna Matching Efficiency

Dielectric loading by the finger on the antenna results in either resonance detuning or mismatch. Figures 7(a) and 7(b) illustrate the average ME at distances of 0.5 mm and 2.5 mm for the 15 GHz antenna, for five different scenarios, i.e., the WU case and four different finger locations. Similarly, Figures 8(a) and 8(b) show the average ME at distances of 0.5 mm and 2.5 mm for the 28 GHz antenna. Same distances have been chosen for both antenna cases to see the effect of ME when the antenna is in close proximity to user. Finally, the average ME for the 60 GHz antenna for the five scenarios is

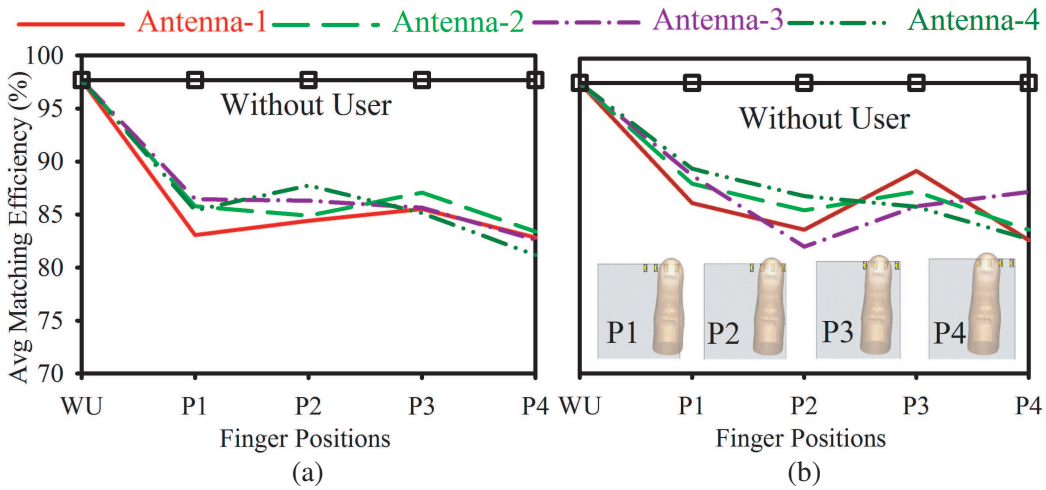

Figure 7. Average matching efficiency when index finger is placed at (a) 0.5 mm and (b) 2.5 mm, from the antenna elements for 15 GHz.

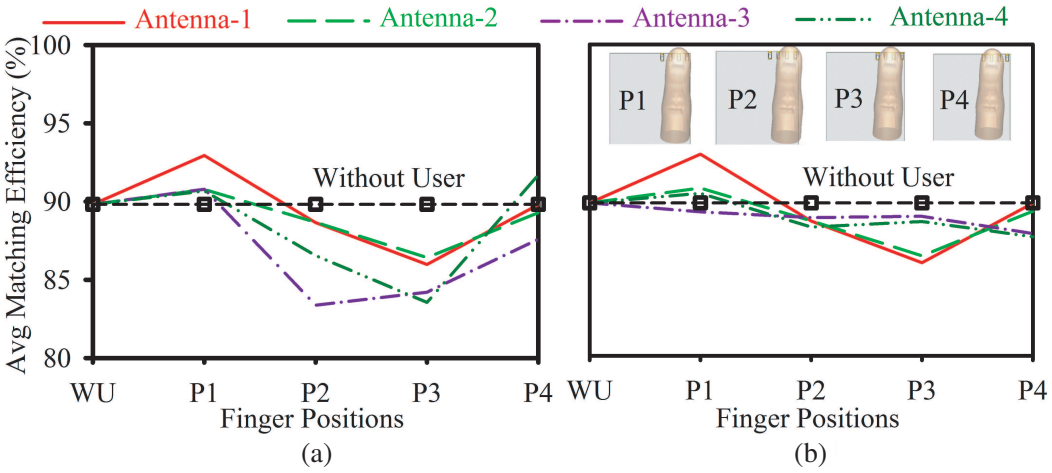

Figure 8. Average matching efficiency when index finger is placed at (a) 0.5 mm and (b) 2.5 mm, from the antenna elements for 28 GHz.

depicted in Figures 9(a) and (b). The reason behind choosing only minimum and maximum distances is to quantify the effects of the finger on the antenna ME at 15, 28 and 60 GHz. It is noticed from Figures 7, 8 and 9 that the ME fluctuates slightly at all frequencies and is not significantly affected by the user finger because of the wider bandwidth of each antenna which still allows the antenna to operate in required frequency region.

4. IMPACT OF USERS ON ANTENNA'S MIMO PERFORMANCE

The deployment of mobile mmWave systems for high speed data communication is expected to be supported by essential antenna-related technologies such as MIMO and diversity techniques. In both systems, the impact of users may strongly affect antenna design parameters. For example, the radiation patterns from these terminal antennas in centimeter and mmWave bands are more directive with a smaller angular spread [18]. Thus, the effects of the propagation environment will be more sensitive to the MIMO performance of mobile terminals in these frequency bands. For MIMO performance in mobile terminals, the considered parameters include ECC and MUX (see Equations (1) and (2)), which

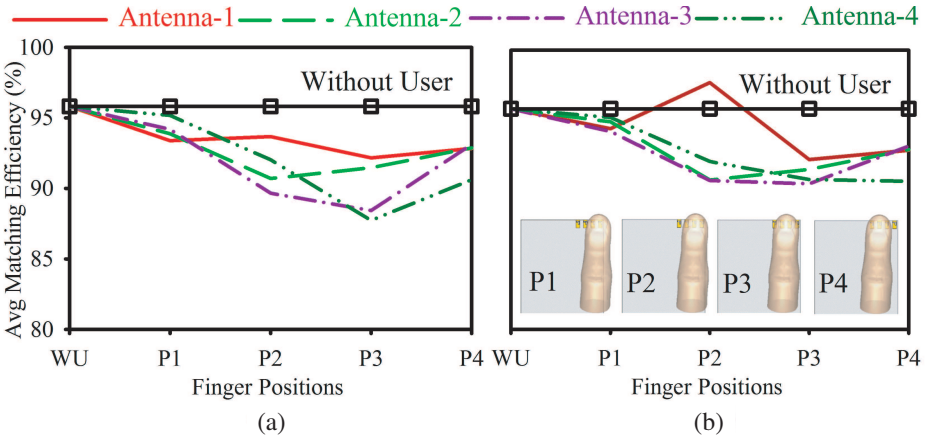

Figure 9. Average matching efficiency when index finger is placed at (a) 0.5 mm and (b) 2.5 mm from the antenna elements for 60 GHz.

are evaluated according to [19, 20];

$$\rho_e = \frac{\oint\oint XPR \times E_{\theta i}(\Omega)E^*_{\theta j}(\Omega)P_\theta(\Omega) + E_{\phi i}(\Omega)E^*_{\phi j}(\Omega)P_\phi(\Omega)d\Omega}{\sqrt{\oint\oint XPR \times G_{\theta i}(\Omega)P_\theta(\Omega) + G_{\phi i}(\Omega)P_\phi(\Omega)d\Omega}\sqrt{\oint\oint XPR \times G_{\theta j}(\Omega)P_\theta(\Omega) + G_{\phi j}(\Omega)P_\phi(\Omega)d\Omega}} \quad (1)$$

where $E_i(\theta, \phi)$ is the complex 3D radiated field pattern for antenna i, XPR the cross polarization field components in the environment, $P_{\theta,\phi}(\Omega)$ the wave distribution of the specific ϕ, θ angular directions, and $G_{\theta,\phi}(\Omega)$ the gain (i.e., $G_\theta(\Omega) = E_\theta(\Omega)E_\theta(\Omega)^*$).

$$\eta_{mux} = \sqrt{\eta_i\eta_j(1 - |m|^2)} \quad (2)$$

where η_{ij} is the total efficiency of ith and jth antennas, and $|m|$ is the magnitude of the complex correlation between the two antennas. Due to its unique expression, MUX is ideal for evaluating the effectiveness of MIMO mobile terminal antennas, as it also yields results consistent with those obtained from link-level performance evaluations of MIMO antennas [21].

4.1. Effect of User's on Antenna ECC and MUX

In this section, the envelop correlation coefficient and multiplexing efficiency of each antenna configuration is calculated by using the simulated embedded far-field radiation patterns in a uniform isotropic environment.

Figures 10, 11, and 12 compare the ECC and MUX assessed in FS (without user) with user for each antenna case. It is observed that the ECC results are well below the maximum limits. Since

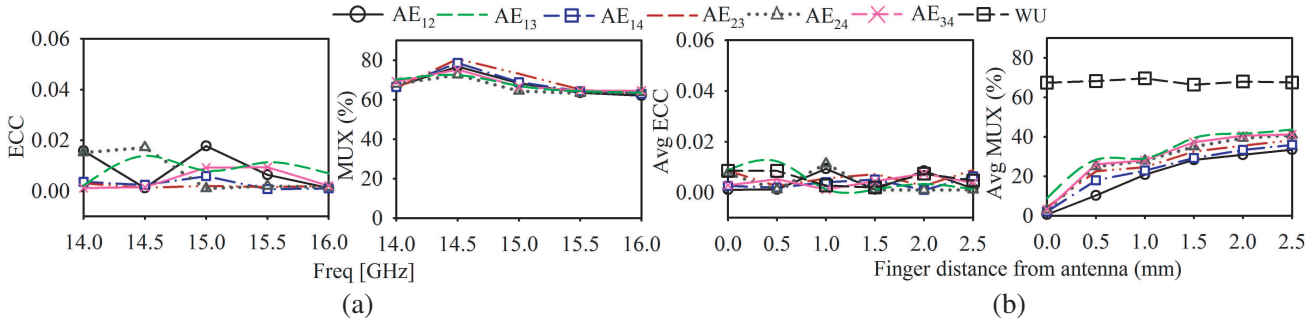

Figure 10. MIMO performance: (a) ECC and MUX in FS, and (b) average ECC and MUX with the variation of the distances between the antenna and the index finger for 15 GHz.

all investigated designs have shown low ECC values in both scenarios (in FS and with user), the MIMO study is then extended to the evaluations of MUX. To effectively consider the user's effects in evaluating MUX, the same user's finger positions on top of the antenna provided in Section 3.1 for RE are considered. The antenna's total efficiency is calculated at the six different finger distances above the antennas. Average ECC and average MUX for different distances from the antenna (0 mm to 2.5 mm) at location P1 for all antennas are shown in Figure 10(b), Figure 11(b), and Figure 12(b). Intuitively, the antenna with degraded total efficiency caused signal-to-noise (SNR) reduction of the received signals. This affects MUX, which is dependent on the ECC and total efficiency of the antenna elements [20]. For all cases, MUX is observed to gradually increase with the increase of the distance of user's index finger. Meanwhile, Figures 13 and 14 show the average values of ECC and MUX for different finger variations (2 mm for 15 GHz, 1.5 mm for 28 and 60 GHz) on top of antenna elements. It is seen that very low ECC

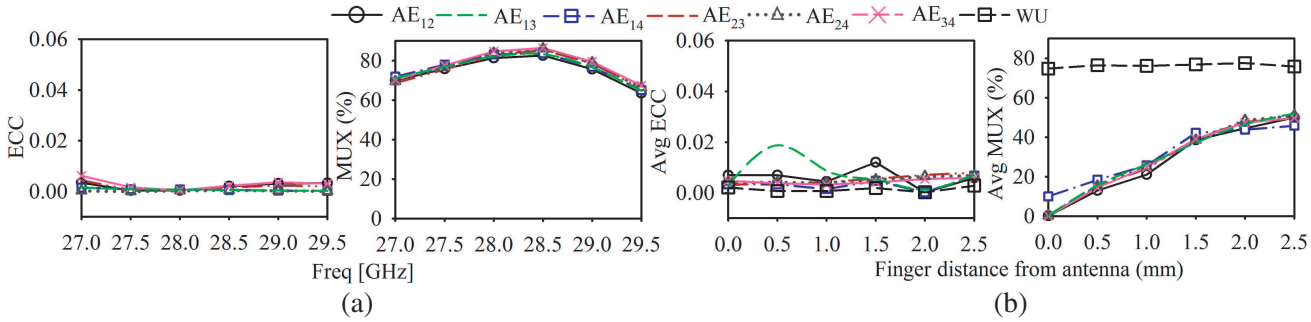

Figure 11. MIMO performance: (a) ECC and MUX in FS, and (b) average ECC and MUX with the variation of the distances between the antenna and the index finger for 28 GHz.

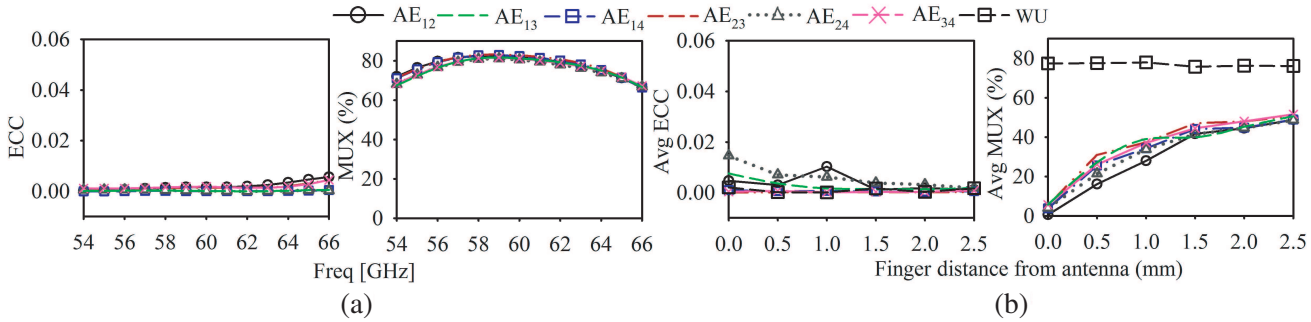

Figure 12. MIMO performance: (a) ECC and MUX in FS, and (b) average ECC and MUX with the variation of the distances between the antenna and the index finger for 60 GHz.

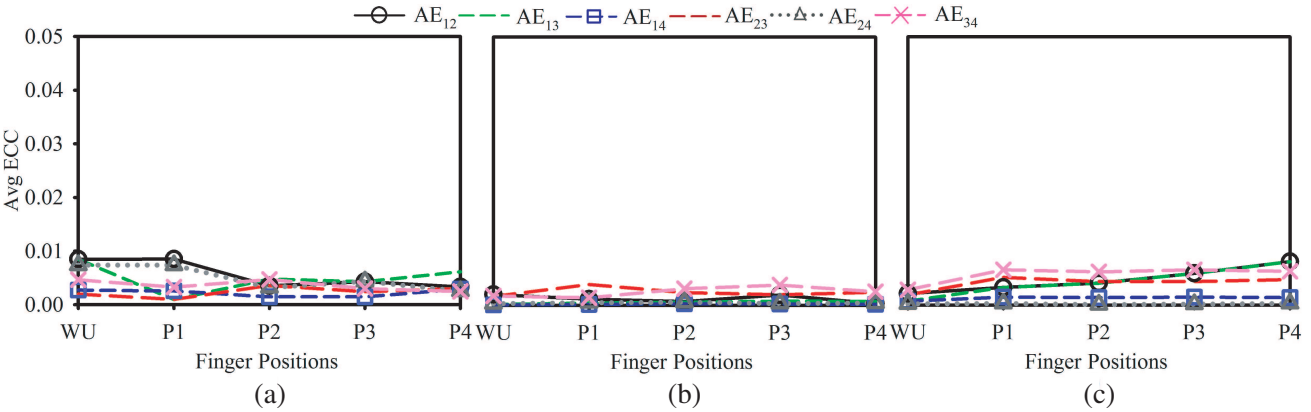

Figure 13. Average envelop correlation coefficient with the variation of finger position: (a) 2 mm at 15 GHz, (b) 1.5 mm at 28 GHz, and (c) 1.5 mm at 60 GHz.

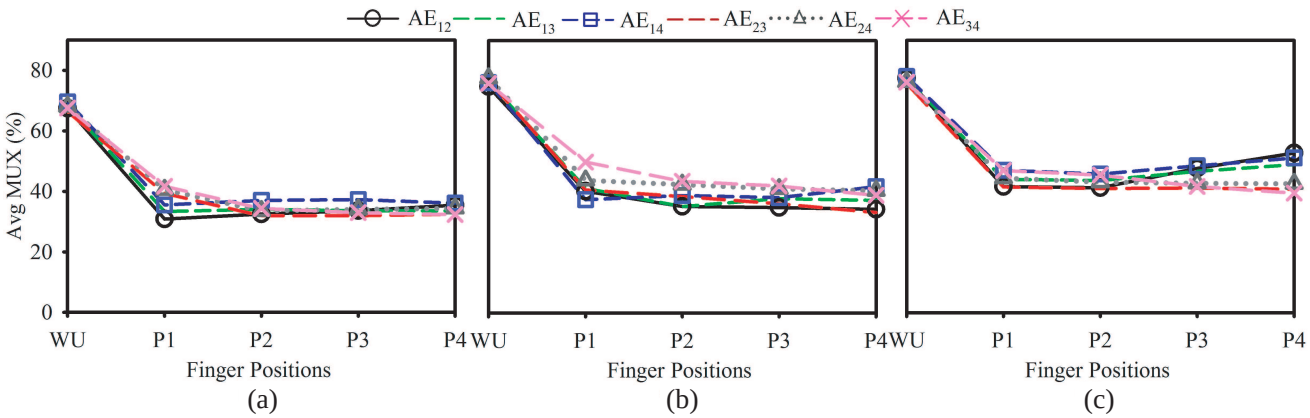

Figure 14. Average MUX with the variation of finger position: (a) 2 mm at 15 GHz, (b) 1.5 mm at 28 GHz, and (c) 1.5 mm at 60 GHz.

values are obtained for such antenna cases, indicating that such particular clearance between antenna and user's index finger enables moderate amount of energy radiation.

5. CONCLUSION

In this study, the user effect on a 4-port planar antenna designed for 15 GHz, 28 GHz and 60 GHz mobile terminal antennas is investigated in terms of S-parameter, average RE, average ME and MIMO parameters such as ECC and MUX. The antenna operating frequency is seen to be shifted, along with bandwidth variation, when the index finger is close to the antenna at all frequencies. The antenna RE is observed to be severely decreased with a closer finger-to-antenna distance due to the shadowing by the index finger. This has also caused the decrease in MUX for all antennas. Significant RE and MUX reductions are found when the index finger is placed at a distance between 0 and 2 mm (for 15 GHz), and between 0 and 1.5 mm (for 28 and 60 GHz). This insight allows the designers to effectively enumerate and address key parameters in designing mmWave antennas for mobile terminals in typical user's scenarios.

Thus, it will be critical to have at least 1.5 or 2 mm clearance for mmWave antennas intended to be used in the vicinity of users. However, it is also observed that the ME and ECC of mmWave antennas are not significantly affected by the user finger but fluctuate slightly. In the near future, this investigation can be extended to fabrication of the proposed antennas and measurements using a realistic finger phantom model.

ACKNOWLEDGMENT

This research was supported financially by the Ministry of Science, Technology and Innovation under eScience fund (Grant No.: 01-01-015-SF0258).

REFERENCES

1. Ying, Z., K. Zhao, T. Bolin, J. Helander, D. Sjöberg, S. He, A. Scannavini, L. J. Foged, and G. Nicolas, "Study of phased array in UE for 5G mm wave communication system with consideration of user body effect," *10th European Conference on Antennas and Propagation (EuCAP)*, 1–2, IEEE, April 2016.
2. El Shorbagy, M., R. M. Shubair, M. I. AlHajri, and N. K. Mallat, "On the design of millimetre-wave antennas for 5G," *16th Mediterranean Microwave Symposium (MMS)*, 1–4, IEEE, November 2016.
3. Liu, J., A. Vosoogh, A. U. Zaman, and J. Yang, "Design and fabrication of a high-gain 60-GHz cavity-backed slot antenna array fed by inverted microstrip gap waveguide," *IEEE Transactions on Antennas and Propagation*, Vol. 65, No. 4, 2117–2122, 2017.

4. Zhou, R., D. Liu, and H. Xin, "A wideband circularly polarized patch antenna for 60 GHz wireless communications," *Wireless Engineering and Technology*, Vol. 3, 97–105, June 2012.
5. Chen, X., L. Tian, P. Tang, and J. Zhang, "Modelling of human body shadowing based on 28 GHz indoor measurement results," *84th Vehicular Technology Conference (VTC-Fall)*, 1–5, IEEE, 2016.
6. Manabe, T., Y. Miura, and T. Ihara, "Effects of antenna directivity and polarization on indoor multipath propagation characteristics at 60 GHz," *IEEE Journal on Selected Areas in Communications*, Vol. 14, No. 3, 441–448, 1996.
7. Zhao, K., C. Gustafson, Q. Liao, S. Zhang, T. Bolin, Z. Ying, and S. He, "Channel characteristics and user body effects in an outdoor urban scenario at 15 and 28 GHz," *IEEE Transactions on Antennas and Propagation*, Vol. 65, No. 12, 6534–6548, 2017.
8. Karadimas, P., B. Allen, and P. Smith, "Human body shadowing characterization for 60-GHz indoor short-range wireless links," *IEEE Antennas and Wireless Propagation Letters*, Vol. 12, 1650–1653, 2013.
9. Rappaport, T. S., S. Sun, R. Mayzus, H. Zhao, Y. Azar, K. Wang, G. N. Wong, J. K. Schulz, M. Samimi, and F. Gutierrez, "Millimeter wave mobile communications for 5g cellular: It will work!," *IEEE Access*, Vol. 1, 335–349, 2013.
10. Ojaroudiparchin, N., M. Shen, and G. Pedersen, "Multi-layer 5G mobile phone antenna for multi-user mimo communications," *23rd Telecommunications Forum Telfor (TELFOR)*, 559–562, November 2015.
11. Hong, W., K. Baek, Y. Lee, and Y. G. Kim, "Design and analysis of a low-profile 28 GHz beam steering antenna solution for future 5g cellular applications," *MTT-S International Microwave Symposium (IMS)*, 1–4, IEEE, June 2014.
12. Zhao, K., J. Helander, D. Sjöberg, S. He, T. Bolin, and Z. Ying, "User body effect on phased array in user equipment for the 5G mmWave communication system," *IEEE Antennas and Wireless Propagation Letters*, Vol. 16, 864–867, 2017.
13. Dussopt, L., Y. Lamy, S. Joblot, J. Lantri, H. Salti, P. Bar, H. Sibuet, B. Reig, J.-F. Carpentier, C. Dehos, and P. Vincent, "Silicon interposer with integrated antenna array for millimeter-wave short-range communications," *Microwave Symp. Int. MTT-S. Dig.*, IEEE, Montreal, Canada, June 17–22, 2012.
14. Wu, T. T. S. Rappaport, and C. M. Collins, "The human body and millimeter-wave wireless communication systems: Interactions and mplications," *International Conference on Communications (ICC)*, 2423–2429, IEEE, June 2015.
15. Zhadobov, M., N. Chahat, R. Sauleau, C. Le Quement, and Y. Le Drean, "Millimeter-wave interactions with the human body: State of knowledge and recent advances," *International Journal of Microwave and Wireless Technologies*, Vol. 3, No. 2, 237–247, 2011.
16. Heino, M., C. Icheln, and K. Haneda, "Finger effect on 60 GHz user device antennas," *10th European Conference on Antennas and Propagation (EuCAP)*, 1–5, IEEE, April 2016.
17. Li, Y., Y. Luo, and G. Yang, "12-port 5G massive MIMO antenna array in sub-6 GHz mobile handset for LTE bands 42/43/46 applications," *IEEE Access*, 2017.
18. Ying, Z., K. Zhao, T. Bolin, S. He, A. Scannavini, L. J. Foged, and G. Nicolas, "Multiplexing efficiency of high order MIMO in mobile terminal for 5G communication at 15 GHz," *International Symposium on Antennas and Propagation (ISAP)*, 594–595, IEEE, October 2016.
19. Sharawi, M. S., "Current misuses and future prospects for printed multiple-input, multiple-output antenna systems [wireless corner]," *IEEE Antennas and Propagation Magazine*, Vol. 59, No. 2, 162–170, 2017.
20. Tian, R., B. K. Lau, and Z. Ying, "Multiplexing efficiency of MIMO antennas with user effects," *International Symposium on Antennas and Propagation Society (APSURSI)*, 1–2, IEEE, July 2012.
21. Athley, F., A. Derneryd, J. Friden, L. Manholm, and A. Stjernman, "MIMO performance of realistic UE antennas in LTE scenarios at 750 MHz," *IEEE Antennas Wireless Propag. Lett.*, Vol. 10, 1337–1340, 2011.